International Conference on Renewable Energies and Power Quality (ICREPQ'13)
Bilbao (Spain), 20th to 22th March, 2013
Renewable Energy and Power Quality Journal (RE&PQJ)
ISSN 2172-038 X, No.11, March 2013

Comparative Study of Current Controllers for Shunt Active Power Compensators used in Smart Grid Applications

J.C. Alfonso Gil, C. Ariño, H. Beltran, E. Pérez

Department of Industrial Systems Engineering and Design,
Universitat Jaume I de Castelló
Av. Vicent Sos Baynat, s/n 12071 Castellón de la Plana, (Spain)
Phone: +0034 964 72 80 00, e-mail: **jalfonso@uji.es, arino@uji.es, hbeltran@uji.es, pereze@uji.es**

Abstract. This paper presents a comparative study among different current controllers implemented in a Shunt Active Power Compensator (SAPC) to be used in smart grid applications. During the operation of a smart grid, the SAPC should deliver sinusoidal or non-sinusoidal currents to the Point of Common Coupling (PCC), and this current exchange must be precisely controlled. Three current controllers are analysed in this paper. The two first controllers are a hysteresis band controller and a feedforward proportional controller. Both controllers are designed to work in stationary reference frame. The third one is a PI controller implemented in a synchronous reference frame. The results show that the synchronous reference frame PI controller is unable to track currents with a significant harmonic distortion. Conversely, the behavior of the two stationary reference frame controllers remains unaffected by a high harmonic content in the reference currents. Finally, the results also show that among them, the hysteresis bandwidth controller presents the best performance with similar power losses.

Keywords

Smart Grid, Power Quality, Current Controllers, Active Power Compensators.

1. Introduction

Power quality is currently one of the most important global issues due to its influence on the nation's economies [1]. Regulations as well as power quality improvement systems are undergoing a continuous development to promote and achieve better and more efficient electrical systems.

Furthermore, nowadays more and more cogeneration plants are connected to the grid and the number of wind turbines also increases constantly. Same trends are being experiences by small generation technologies, such as micro cogeneration power plants and PV panels.

In this context, in the future the Smart Grids technologies [4]-[6] will play an important role in maintaining reliability of the supply by continuously monitoring and controlling the grid and the generators, achieving this way an improvement in its sustainability and performance when the complexity of electricity distribution increases.

One of the most important techniques in a Smart Grid configuration is the inclusion of Shunt active power compensators (SAPCs) [2], [3]. The configuration of such Smart Grid is shown in Fig. 1.

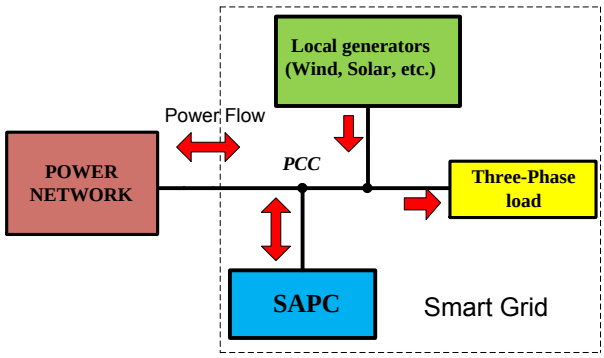

Fig. 1 SAPC connection to power network and to smart grid

In an ideal case, the SAPC supplies to the Smart Grid the non-efficient currents due to reactive power, harmonic distortion, etc., avoiding these currents being delivered by the electrical grid. In this sense, the SAPC would make the whole smart grid appear as an ideal generator or a resistive load to the power network.

However, in a real case the SAPC has a limited power and capacity and therefore can be unable of compensating all the inefficiencies. When this is the case, a selective SAPC, which only compensates some of the inefficiencies, can be used. A way to implement this selective compensation is by means of a current control in the SAPC.

Due to the presence of harmonic distortion in a general case and the limitations of the SAPC, this selective compensation results in a non-sinusoidal current reference given to the SAPC controller.

Taking this operational consideration into account, a comparative analysis among three current controllers to be potentially used to control the SAPC is performed in this paper. The two first controllers are a hysteresis band (HB) and a feedforward proportional controller. Both are

designed to work in a stationary reference frame. Finally, the third controller is a PI controller which has been implemented in a synchronous reference frame (dq0).

The organization of the paper is as follows. In Section 2, two SAPC current controllers (HB and feedforward P) operating in stationary reference frame are presented. In this sense, the system transfer function of the proposed SAPC is firstly obtained from a block diagram. Then, in accordance to the SAPC transfer function, the controller parameters are defined. Section 3 is devoted to introduce a PI current controller working in a synchronous reference frame. Thereafter, some simulation results representing the performance of the controllers under different operation conditions are presented in section 4. And finally, some conclusion remarks are discussed in section 5.

2. Stationary reference frame controllers

In this section, two different controllers that can be used to manage the currents exchanged by a SAPC are proposed. Both controllers are based on stationary reference frame [7].

A. Hysteresis Band controller

Usually, current controllers for AC inverters are hysteresis controllers [8], [9]. This kind of controllers is designed with the objective of obtaining zero phase and magnitude error. To achieve that, the output current of the SAPC is compared with the reference and the output of the controller is switched as an on-off controller with a hysteresis band. This control scheme is shown in Fig. 2.

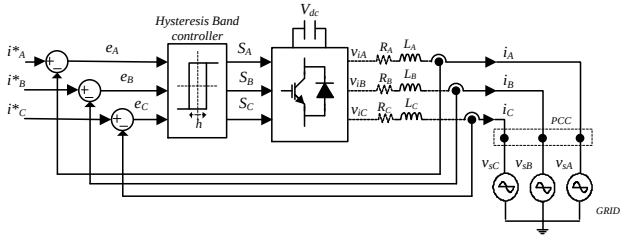

Fig. 2 Hysteresis Band controller

This comparator, while acting as a current controller, generates the switching signals for the power converter. The controller performs the two functions, avoiding the use of an extra modulator block in the control of the SAPC.

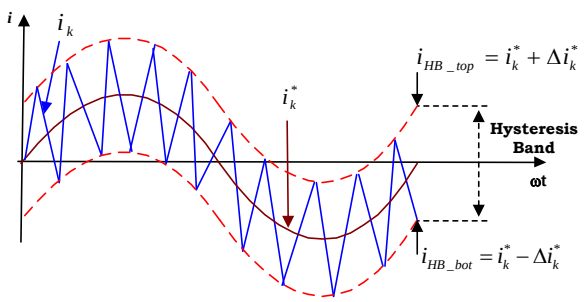

Fig. 3 Hysteresis Band performance

Fig. 3 shows the behaviour of the HB controller. Note how upper and lower limits are obtained for the current by shifting the reference up and down by a given quantity. These are defined as the hysteresis bands. The controller generates the switching signals to keep the SAPC output current inside the limits established by these bands. The values of the upper and lower bands are defined in (1) and (2).

$$i_{HB\_top} = i^*_k + \Delta i^*_k \quad (1)$$

$$i_{HB\_bot} = i^*_k - \Delta i^*_k \quad (2)$$

where Δi defines the limits of Hysteresis Band. The main advantage of this control is the simplicity of the control scheme that provides the system with great sturdiness, obtaining the reference track without errors, regardless of changes in load. On the other hand, a drawback of this control strategy is that the switching frequency of the power converter is variable and unknown, because it depends on the hysteresis band. This is also true for the harmonic distortion.

B. Feedforward controller

The second analysed controller is based on a proportional type controller (P) with feedforward working in stationary reference frame (Fig. 4).

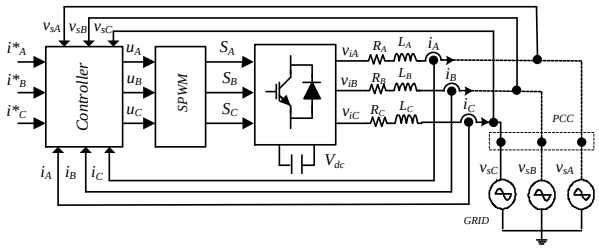

Fig. 4 Feedforward controller

In this case the controller is divided into two different modules (Fig. 5). The first one is a feedforward controller which generates the desired voltages to be applied to the converter according to the defined reference currents. This is done from the model of the plant and in an open loop control scheme. The second module is a proportional controller which has to be able to track the reference currents when they change. Then, a PWM modulator is used to generate the switching signal of power converter as shown in Fig. 4.

From Fig. 4, the voltages and currents in the output of SAPC can be written as in (3).

$$v_{ik} = R \cdot i^*_k + L \cdot \frac{d}{dt} i^*_k + v_{sk} + P(i^*_k - i_k), \quad k = A, B, C \quad (3)$$

Where v_{ik} is the inverter voltage output, v_{sk} is the grid voltage and R-L are the values of the reactance of L-Filter.

https://doi.org/10.24084/repqj11.273 257 RE&PQJ, Vol.1, No.11, March 2013

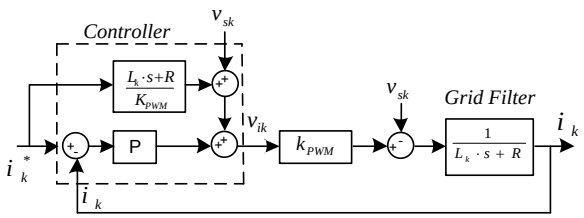

Fig. 5 Feedfordward control diagram block

The proportional controller P can be obtained forcing a damping factor of ξ =0.707 and a settling time of $t_{st} = 2$ ms. Using the characteristic equation (4).

$$1 + PG_{OL}(s) = 1 + K \cdot k_{PWM} \cdot \frac{1}{R + L_k \cdot s} = 0 \tag{4}$$

$$|K| = \left. \frac{|R + L_k \cdot s|}{k_{PWM}} \right|_{s=-4/t_{st}} = 11.6 \tag{5}$$

3. Synchronous reference frame controller

Fig. 6 shows a three-phase inverter connected to grid, where a reactance is connected between the electronic power converter and the Grid. The DC-Bus is considered an ideal voltage DC source. Using the Clarke and Park transformations [10], [11] the vector projections of three phase currents on a reference system rotating at synchronous speed are obtained. The synchronous speed corresponds to the pulsation of the fundamental voltage component. With this transformation, the fundamental component of the space vector resulting phase system loses its temporal dependence. Thus, in steady state, its projections on the d and q axes are constant in time. Consequently, a current controller based on PI controllers will be able to reduce to zero steady state errors.

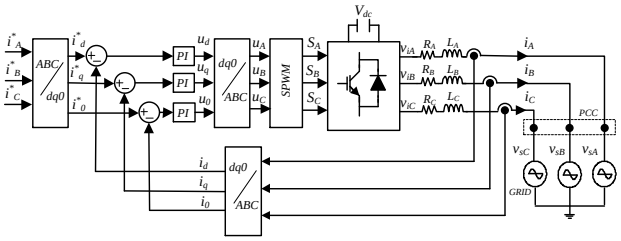

Fig. 6 Synchronous reference frame (*dq0*) control with PI controllers

From Fig. 6, the voltages and currents in the system can be written as (6).

$$v_{ik} = R \cdot i_k + L \cdot \frac{d}{dt} i_k + v_{sk}, \quad k = A, B, C \tag{6}$$

Where v_{ik} is the inverter voltage output, v_{sk} is the grid voltage and R-L are the values of the reactance of L-Filter.

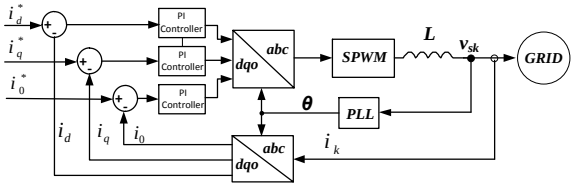

Fig. 7 *dq0* control diagram block

Fig. 8 shows the block diagram of the closed-loop system used to design the PI controller.

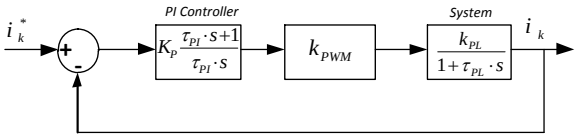

Fig. 8 Closed loop control

The open loop transfer function of system can be written as

$$G_{OL}(s) = K_P \frac{\tau_{PI} \cdot s + 1}{\tau_{PI} \cdot s} \cdot k_{PWM} \cdot \frac{k_{PL}}{1 + \tau_{PL} \cdot s} \tag{7}$$

where:

$$\tau_{PL} = \frac{L}{R}; k_{PL} = \frac{1}{R}; \qquad k_{PWM} = 1.$$

In order to obtain a suitable response of the closed-loop system, a damping factor of ξ =0.707 and a settling time of $t_{st} = 2$ ms. are required. To achieve them, root locus design techniques are used (Fig. 9), giving the K_p and K_i values of the PI controller shown in (8).

$$\begin{aligned} K_P &= 22.92 \\ K_I &= 45773 \end{aligned} \tag{8}$$

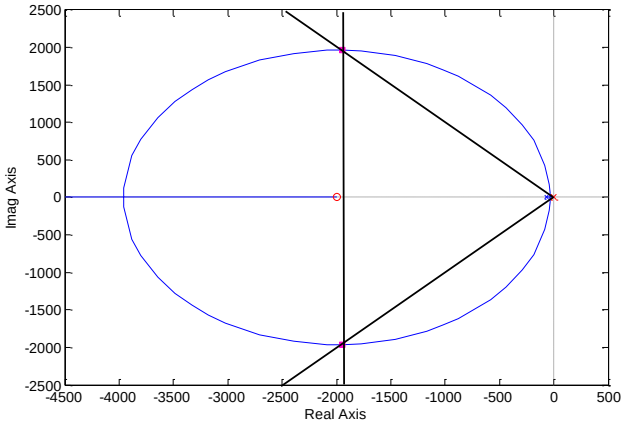

Fig. 9 Root locus, design specifications and closed-loop poles of the system.

4. Simulation results and discussion

To analyse the performance of each of the proposed controllers, a series of simulations have been carried out on Matlab Simulink and its toolbox SimPowerSys.

Table I summarizes the values of the system parameters and those of the controllers configuration used along the simulations.

As previously discussed, the current references provided to the SAPC in a general case will be non-sinusoidal, and therefore the controllers' response will be evaluated under those circumstances. In particular, the analysis is performed for the case of a current reference with a fundamental harmonic with an amplitude of 20 A and a 7th harmonic with an amplitude of 2 A.

https://doi.org/10.24084/repqj11.273 258 RE&PQJ, Vol.1, No.11, March 2013

Table I Simulation Parameters

Parameter	Description	Value
L	Inductor filter	6mH
R	Inductor resistance	400mΩ
F_{PWM}	PWM carrier Frequency	20250 Hz
f	Grid frequency	50±1Hz
Vb	Line-to-Line RMS Voltage	400V
Vdc	DC Bus Voltage	800V
Kp	Proportional constant	18.82
Ki	Integral constant	28956
K_{PWM}	Gain of PWM inverter	1
P	Gain of feedfordware reg.	11.6
I^*	Amplitude of reference current	20 A
Δi_k^*	Hysteresis bandwidth	0.4 A
t_s	Switching time of the IGBTs	0.09 μs.

Furthermore, for comparison purposes, the controllers' response to a sinusoidal reference has been also studied. This is the case arising when the inefficiencies of the smart grid are only associated to the consumption of reactive power.

In order to evaluate the performance of each of the proposed current controllers, three different parameters are calculated:

A. The Integral Absolute Error (IAE) per cycle:

$$IAE = \int_{t_0}^{t_0+T} \left| i^*(t) - i(t) \right| dt \qquad (9)$$

This parameter quantifies the tracking error of the controlled system throughout a grid voltage period.

B. The harmonic distortion introduced by the control system:

$$HD(i) = \frac{\sqrt{\sum_{k=2}^{\infty} (i_k - i_k^*)^2}}{i_1} \qquad (10)$$

where i_k represents the current harmonic of order k. This parameter is calculated as the distortion produced by the harmonics which do not appear in the reference signal: It from the standard THD in the fact that the harmonic content of the reference is eliminated here from the calculation.

C. Power losses in the converter. These losses are due to the IGBTs' switching and can be estimated as:

$$P_s = \frac{3}{\pi} V_{dc} I^* t_s f_{pwm} \qquad (11)$$

The implementation of the three different controllers in the SimPowerSys framework is shown from Fig. 10 to Fig. 12.

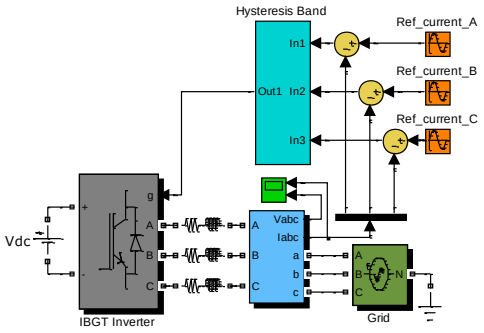

Fig. 10. Diagram block for the hysteresis band controller

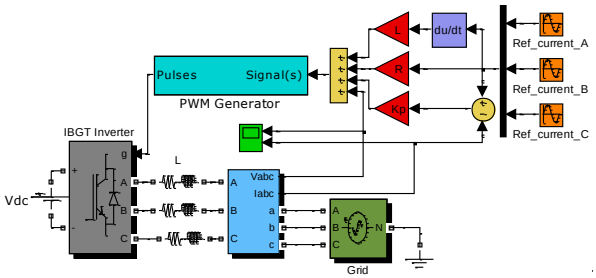

Fig. 11 Diagram block for the feedforward controller

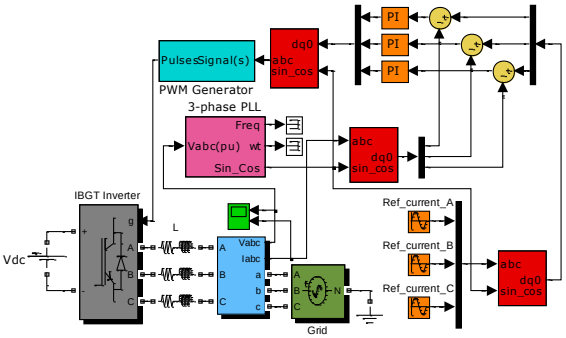

Fig. 12 Diagram block for synchronous reference frame PI controller

In a first set of simulations, sinusoidal current references with amplitude of 20A have been used. The system responses obtained with the three different controllers are shown from Fig. 13 to Fig. 15. As can be seen all the controllers are able to track the reference with a settling time of around 2 ms.

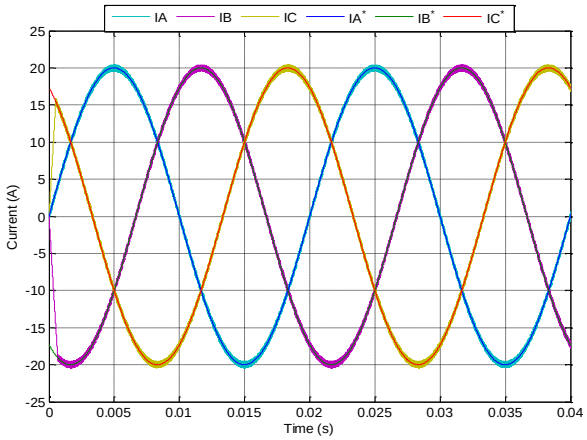

Fig. 13 SAPC output currents for the HB controller with sinusoidal reference

https://doi.org/10.24084/repqj11.273 259 RE&PQJ, Vol.1, No.11, March 2013

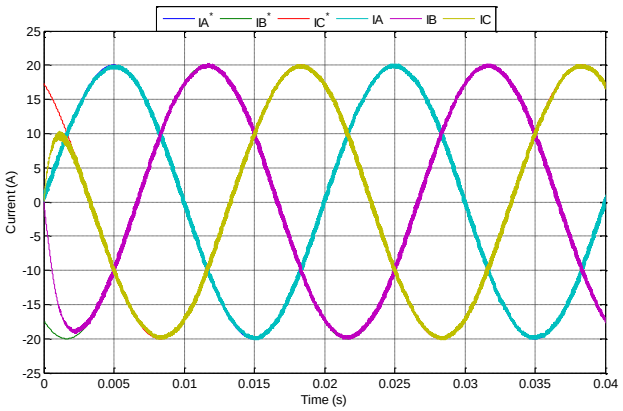

Fig. 14 SAPC output currents for the feedforward controller with sinusoidal reference

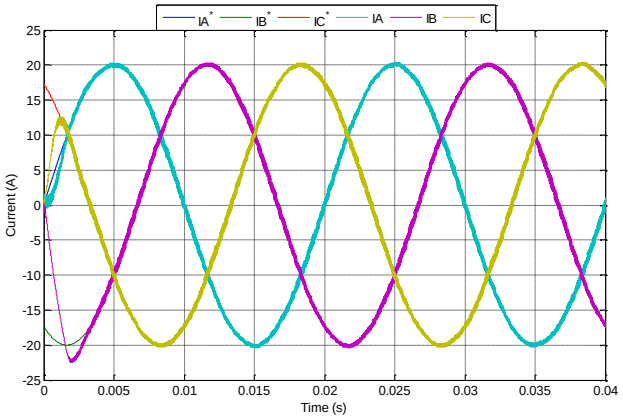

Fig. 15 SAPC output currents for the dq0 controller with sinusoidal reference

After that, the control strategies have been evaluated with the proposed non-sinusoidal current reference. Fig. 16, Fig. 17 and Fig. 18 show the corresponding simulation results. In this case, it can be observed how the behavior of the stationary reference frame controllers remain unaffected by the harmonic distortion on the demanded currents (I*) and are still able to follow them with a similar settling time. However, the synchronous reference frame controller shows a worst tracking of the reference.

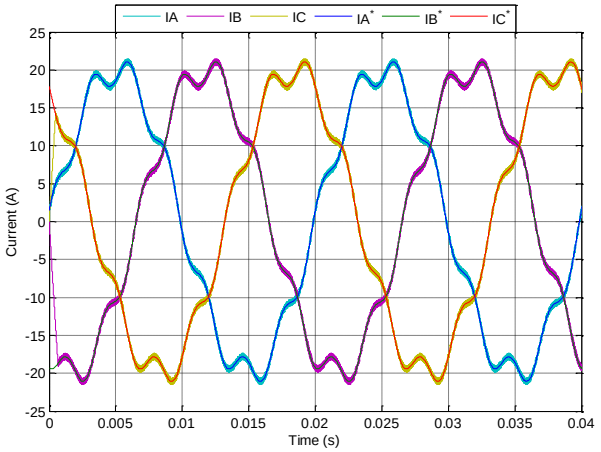

Fig. 16 SAPC output currents for the HB controller with non-sinusoidal reference

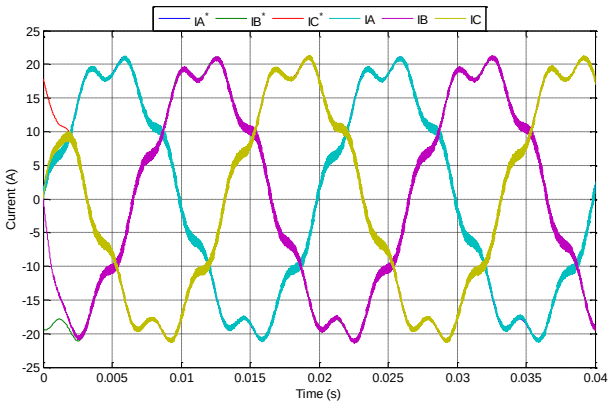

Fig. 17 SAPC output currents for the feedforward controller with non-sinusoidal reference

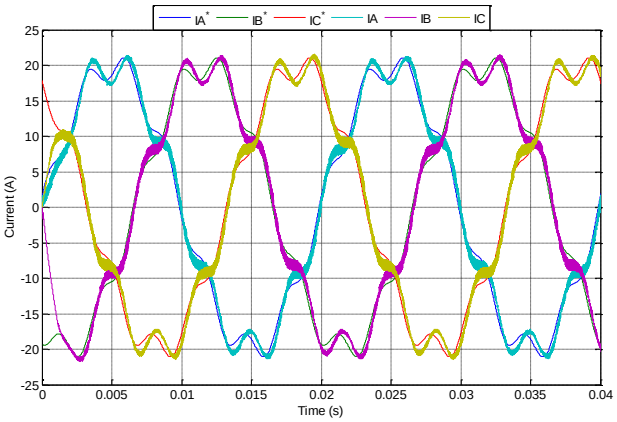

Fig. 18 SAPC output currents for the dq0 controller with non-sinusoidal reference

Table II and III summarize the previously introduced values of IAE per cycle, HD and power losses obtained for each of the proposed current controllers. For the dq0 controller, unlike the other two controllers, the IAE and the HD obtained for the non-sinusoidal references is significantly worse than that obtained for the sinusoidal reference. This is due to the fact that, because of the harmonic content of the current references, the PI controllers' performance, operating in a synchronous reference frame, is limited.

Table II Sinusoidal reference currents

Current controller	IAE	HD	P. losses(W)
Hysteresis Band (HB)	0.0044	0.0180	30.0
Feedforward	0.0058	0.0242	27.5
dq0	0.0054	0.0242	27.5

Table III Non-sinusoidal reference currents

Current controller	IAE	HD	P. losses(W)
Hysteresis Band (HB)	0.0044	0.0180	30.0
Feedforward	0.0058	0.0242	27.5
dq0	0.180	0.0736	27.5

Therefore, it can be finally concluded from the comparison of the controllers' performances that the hysteresis band controller presents the best behavior, out of the three analyzed, in terms of IAE and HD while it presents similar degrees of power losses.

https://doi.org/10.24084/repqj11.273

5. Conclusions

The results obtained in this paper show how any of the proposed current controllers can track sinusoidal references, presenting all of them similar degrees of accuracy. However, important differences arise when the SAPC has to inject currents with significant harmonic distortion. In this case, the synchronous reference frame PI controller is clearly unable to track such currents. On the contrary, the behavior of both the stationary reference frame controller and that of the hysteresis bandwidth controller remain unaffected by the harmonic content of the reference currents, being the latter the one presenting the best performance with similar power losses.

Acknowledgement

This work is included within the project "Development and implementation of control strategies for a compensator-generator system in Smart Grid applications", with reference P1·1A2011-12 supported by the Universitat Jaume I de Castelló and the Fundació Caixa Castelló-Bancaixa.

References

[1] Tianqing Sun, Xiaohua Wang, Xianguo Ma., "Relationship between the economic cost and the reliability of the electric power supply system in city: A case in Shanghai of China" *Appl Energy*, vol. 86, pp. 2262-2267, Oct. 2009

[2] S. Orts-Grau, F.J. Gimeno-Sales, S. Segui-Chilet, A. Abellan-Garcia, M. Alcañiz-Fillol, and R. Masot-Peris, "Selective compensation in four-wire electric systems based on a new equivalent conductance approach," *IEEE Trans. Ind. Electron.*, vol. 56, no. 8, pp. 2862–2874, Aug. 2009

[3] B. Sing and V. Verma, "Selective Compensation of Power-Quality Problems through Active Power Filter by Current Decomposition," *IEEE Trans. Power Del.*, vol. 23, no. 2, pp. 792–799, Mar. 2008.

[4] H. Slootweg, "Smart Grids- The future or fantasy," *Smart Metering - Making It Happen, 2009 IET*, pp. 1–19, Feb. 2009

[5] M. Hashmi, S. Hänninen, K. Mäki, "Survey of Smart Grid Concepts, Architectures and Technological Demonstrations Worldwide," *Innovative Smart Grid Technologies (ISGT Latin America), 2011 IEEE PES Conference on*, pp. 1–7, Oct. 2011

[6] Fangxing Li, Wei Qiao, Hongbin Sun, Hui Wan, Member, Yan Xia, Member, Zhao Xu, Pei Zhang, "Smart Transmission Grid: Vision and Framework," *IEEE Trans. Smart Grid*., vol. 1, pp. 168–177, Sept. 2010.

[7] Daniel Nahum Zmood, Donald Grahame Holmes. "Stationary Frame Current Regulation of PWM Inverters With Zero Steady-State Error" *IEEE Transactions On Power Electronics*, Vol.18, No.3, May 2003.

[8] S. R. Prusty, S. K. Ram, B. D. Subudhi, K. K. Mahapatra, "Performance analysis of adaptive band hysteresis current controller for shunt active power filter," *Emerging Trends in Electrical and Computer Technology (ICETECT), 2011 International Conference on*, pp. 425–429, Mar. 2011.

[9] M. Mohapatra, B. C. Babu, "Fixed and sinusoidal-band hysteresis current controller for PWM voltage source inverter with LC filter," Students' Technology Symposium, 2010 IEEE , pp. 88–93, Apr. 2010.

[10] E. Clarke, Circuit Analysis of AC Power Systems, vol. 1, 2nd edition, pp. 81, Wiley Publications, 1950.

[11] R. H. Park, "Two reaction theory of synchronous machines. Generalized method of analysis – Part I", *Proceedings Winter Convention of AIEE*, pp. 716-730, 1929